Trop J Nat Prod Res, December 2023; 7(12):5587-5594

ISSN 2616-0684 (Print)
ISSN 2616-0692 (Electronic)

Tropical Journal of Natural Product Research

Available online at https://www.tjnpr.org

Original Research Article

Exploring the Molecular Interactions between Volatile Compounds in Coconut Shell Liquid Smoke and Human Bitter Taste TAS2R46 Based on the Molecular Docking and Molecular Dynamics

Hamidah Rahman[1], Muhamad Ilham Bintang[2], Aiyi Asnawi[2], Ellin Febrina[3]*

[1]*Department of Public Health, Faculty of Health Sciences, Universitas Muhammadiyah Maluku Utara. Jl. KH. Ahmad Dahlan No. 100 Ternate 97719, North Maluku, Indonesia*
[2]*Faculty of Pharmacy, Universitas Bhakti Kencana, Jl. Soekarno Hatta No.754, Bandung, West Java, 40617, Indonesia.*
[3]*Department of Pharmacology and Clinical Pharmacy, Faculty of Pharmacy, Universitas Padjadjaran, Sumedang 45363, West Java, Indonesia.*

ARTICLE INFO

Article history:
Received 22 October 2023
Revised 12 December 2023
Accepted 13 December 2023
Published online 01 January 2024

ABSTRACT

TAS2R46, a bitter taste receptor, is crucial for detecting harmful substances. Understanding its molecular interactions with bitter compounds could help develop bitter taste modulators for the food and pharmaceutical industries. However, such interactions had remained underexplored. A computational method was utilized in this investigation to examine the binding interactions between TAS2R46 and the bitter components of liquid smoke. By utilizing molecular docking and molecular dynamics simulations, one may analyze the modes of binding, the stability of these interactions, and the essential residues at the binding site. The human TAS2R46 protein (PDB ID 7XP6) had been selected for this study. Molecular docking was employed to predict the binding modes and affinity of the liquid smoke's ligands to the TAS2R46 receptor. Subsequently, molecular dynamics simulations were conducted to analyze the stability and dynamics of the TAS2R46-liquid smoke ligand complexes over a 100 ns timeframe. Our computational findings revealed that the nine teen-reported compounds of liquid smoke could indeed bind to TAS2R46. Delta energy component calculations had indicated the stability of these ligand-receptor complexes, with 1-(2,4,6-trihydroxyphenyl)-ethanone showing the most favorable binding energy. These results provided crucial insights into the molecular basis of bitter taste perception and may have implications for the food industry and drug development. In conclusion, this research bridged a critical knowledge gap by providing a molecular-level understanding of how TAS2R46 interacted with bitter compounds in liquid smoke.

***Keywords*:** TAS2R46, Bitter taste, Liquid smoke, Molecular docking, Molecular dynamics

Introduction

Liquid smoke is a food additive that imparts a distinctive smoky flavor to meat and fish. It is produced by heating wood or biomass in an oxygen-deficient environment for 450–600 degrees Celsius before allowing it to condense into a liquid. Liquid smoke, which ranges in color from yellow to red and is water-soluble, is utilized as an alternative to wood smoke in cooking while preserving the flavor.[1] Liquid smoke is a versatile flavoring agent that can be applied topically to meat and vegetables, serving as a common substitute for the direct infusion of food through wood smoking. Originally, liquid smoke was not marketed or sold as a food additive, but rather as a preservative. By passing smoke from smoldering woodchips through a condenser, which rapidly cools the vapors and causes them to liquefy, liquid smoke is produced. The liquid entraps the water-soluble flavor compounds present in the smoke, whereas a sequence of filters eliminates the insoluble tars and resins.[2] Liquid smoke is a natural product made from condensing the smoke from burning wood.

*Corresponding author. E mail: ellin.febrina@unpad.ac.id
Tel: +62 22 7796200

Citation: Rahman H, Bintang MI, Asnawi A, Febrina E. Exploring the Molecular Interactions between Volatile Compounds in Coconut Shell Liquid Smoke and Human Bitter Taste TAS2R46 Based on the Molecular Docking and Molecular Dynamics. Trop J Nat Prod Res. 2023; 7(12):5587-5594. http://www.doi.org/10.26538/tjnpr/v7i12.31

Official Journal of Natural Product Research Group, Faculty of Pharmacy, University of Benin, Benin City, Nigeria.

The application of liquid smoke has several advantages over traditional smoking methods, including time and energy savings, environmental friendliness, elimination of potentially toxic compounds, and precise control over the smoke flavor. Liquid smoke can be used on any dish to impart smoky flavor, and it is used extensively by food manufacturers as a flavor additive. Additionally, liquid smoke removes harmful compounds associated with traditional smoking methods.

There are limitations to the use of liquid smoke as a flavoring agent, as the smoky flavor of liquid smoke products is not as natural and robust as the traditional flavor. While research has been undertaken to investigate individual taste receptors (e.g., umami, sweet, bitter, and salty receptors) and taste-activating components capable of stimulating receptors, insufficient attention has been paid to the mechanisms underlying the perception of multiple flavors and tastes.[3] The percentage of brine and liquid smoke had a substantial impact on the smoked flavor of Mediterranean mussels; therefore, an investigation was conducted to determine how to optimize the steaming with liquid smoke smoking process.[4] Sensory determinants, encompassing flavor, texture, and taste, exert a significant influence on consumer meal selection. One of the most influential aspects of sensory quality that has a direct impact on customers' food selection is flavor.

Coconut shell liquid smoke is a byproduct of the pyrolysis process of burning coconut shells. It is used as a flavoring agent and preservative in the food industry. The volatile constituents of liquid smoke produced from coconut shells during pyrolysis at a portion of 350-420 °C were assessed in this work.[5] Using GC-MS, another study identified the chemical components of the three distinct grades of liquid smoke from coconut shells.[6] Various chemical compounds in coconut shell liquid smoke were identified, including polyphenols,

polycyclic aromatic hydrocarbons (PAHs), phenol, guaiacol, and EMP compounds.[7] The findings of these studies may be useful in determining the potential applications of different grades of coconut shell liquid smoke.

G proteins and G protein-coupled receptors mediate bitter transduction in mammalian taste receptor cells, according to several biochemical and physiological studies. The family of over 30 bitter taste receptor genes is responsible for imparting bitter taste in animals. Its primary role is to safeguard the organism from the absorption of hazardous substances.[8] The sense of taste is responsible for detecting and distinguishing between sweet, bitter, sour, salty, and amino acid (umami) stimuli, and the discriminatory power of taste is achieved by the activation of different combinations of taste receptors.[9] Bitter taste receptors are type II taste receptor cells (TRCs), which are a subfamily of GPCRs containing a separate population of bitter detecting cells. Taste biology has devoted a substantial amount of effort to elucidating the variation among bitter taste receptors and their agonists.[10] Taste receptors are responsible for detecting and distinguishing between different taste modalities, and the discriminatory power of taste is achieved by the activation of different combinations of taste receptors.

Human bitter taste perception is mediated by 25 bitter taste receptors (T2Rs), which are activated by a wide range of compounds, including smoked liquid. T2Rs are expressed in extraoral tissues, including nasal epithelium, brain, large intestine, testis, and human airways. A study analyzed the expression of TAS2R genes in different extraoral tissues and found a specific pattern of TAS2R expression, mostly independent of tissue origin and the pathological state, except in cancer cells. The study also assessed the functionality of the expressed T2Rs in these cells, measuring intracellular calcium mobilization after stimulation with the bitter compound quinine.[11] A better understanding of the T2R-ligand of smoked liquid interactions can provide novel tools for modulating receptor function in various physiological and pathophysiological conditions. Although research has been undertaken to examine individual bitter taste receptors and the effects of smoked liquid components' smoky tastes on activating these receptors, the mechanisms behind the experience of bitterness remain inadequately understood.

To study the interaction between compounds of smoked liquid and human taste bitter receptors, molecular docking, and molecular dynamics studies can be conducted. A model can be used to predict the affinities between smoked flavor components as ligands and the human bitter taste receptor, based on the synergy of the multiple linear regression, molecular docking, and electronic tongue.[12] Molecular docking and molecular dynamics simulations have been used to characterize the interaction of steviol glycoside (SG) with human bitter taste receptors at the molecular level. The results showed that SG has only one site for orthosteric binding to these receptors, and the binding free energy between the receptor and SG was negatively correlated with SG bitterness intensity.[13] However, the connection between smoked flavor components and bitter taste receptors in humans as ligands has yet to be investigated. A computational method for analyzing the binding interactions between TAS2R46 and the bitter components of liquid smoke is presented in this paper. The investigation incorporated molecular dynamics simulations and molecular docking techniques to examine the binding mechanisms, identify critical residues located in the binding locations, and assess the stability of these interactions.

Materials and Methods

Hardware

The molecular docking and molecular dynamics simulations were performed using an HP Z640 WorkStation Server with the following specifications: 32 GB of random-access memory (RAM), a single Intel Xeon E5-2667 processor, an Nvidia® RTX 3060 graphics processing unit (GPU), and a dual system running Ubuntu 22.04 LTS and Windows 10 Pro-64-bit.

Software

Several software tools were employed in the research to build the studying the molecular interactions between liquid smoke chemicals and human bitter taste TAS2R46 based on molecular docking and molecular dynamics. PyRx 9.0[14] is a free and open-source software that is based on AutoDock and was used for molecular docking. Avogadro[15] is a free and open-source application for editing and visualizing molecular structures. A piece of software called Discovery Studio Visualizer 2021[16], is used for viewing and studying the structures and characteristics of molecules.

Preparation of enzyme structure

TAS2R46 macromolecule (PDB ID 7XP6), which was received from the website https://www.rcsb.org, was the docking target protein. The appropriate target protein was downloaded in *.pdb format. It was then created using Discovery Studio Visualizer 2021 after being initially stripped of all atoms, molecules, and ions that included water. After being isolated from its native ligand (strychnine), the macromolecular structures were then saved in *.pdb format.

Preparation of ligands

Nineteen reported volatile compounds in coconut shell liquid smoke[5] were retrieved from the website pubchem.ncbi.nlm.nih.gov. All the ligand structures were converted and saved in *.pdb format.

Validate the molecular docking procedure

To validate the molecular docking method, strychnine, the native ligand, was re-docked into the binding pocket of the TAS2R46 macromolecule (PDB ID 7XP6). In a cycle of the ligand, the grid box was set to 40:40:40 Å sizes until the binding site was covered and the grid center was formed. Ten GA-run settings in all, ten quick evaluations, and a maximum evaluation of 250,000 were used for validation. Data on binding energy and RMSD were included in the *.dlg file that contained the collected results. Then, using Discovery Studio Visualizer 2021 software, the bonding interactions between the native ligand and macromolecules were displayed. The pre-native ligand and the post-native ligand overlapped. The similarity or suitability of the obtained results was next assessed. The validation was deemed successful if the RMSD value was less than 2.0.

Molecular docking simulation

The nineteen reported volatile compounds in coconut shell liquid smoke[5] docked using AutoDock 4.2 by using the docking parameters were determined using the dimensions and coordinates received during the docking procedure's validation stage.

Scoring and results interpretation

AutoDock assessed the generated binding postures based on energy estimations after the initial docking. The binding poses with the lowest binding energy were identified as the most favorable. The binding poses with the lowest binding energy were identified as the most favorable. A comprehensive analysis of the docking results was carried out to determine the optimal ligand binding poses and to assess the orientations of the ligands within the binding site by utilizing a Discovery Studio Visualizer 2021. This analysis provided insights into the ligand-receptor interactions and the affinity of the ligands for the receptor.

Result and Discussion

Human bitter taste TAS2R46 is a bitter taste receptor that responds to a broad spectrum of bitter substances, but strychnine is the most potent agonist identified.[17] There are 25 known T2Rs in humans responsible for bitter taste perception.[18] Molecular docking and molecular dynamics simulations were employed in this investigation to analyze the interactions between bitter taste receptors and nineteen volatile chemicals present in liquid smoke derived from coconut shells.

Molecular docking

Validation for docking procedure

The successful redocking of strychnine and the low RMSD indicate that the chosen docking procedure and software can accurately predict the binding mode of this ligand with TAS2R46. This is crucial for various applications, including drug discovery, where the ability to

ISSN 2616-0684 (Print)
ISSN 2616-0692 (Electronic)

predict how a small molecule interacts with a target receptor is essential for designing and optimizing new drug candidates.
A low RMSD indicates that the docking procedure was successful in reproducing the correct binding pose. By using location of the binding site with a grid box size of 40 Å × 40 Å × 40 Å with coordinates -21.727 Å, -6.323 Å, and -5.281 Å obtained an RMSD value of 1.628 Å (Figure 1). The obtained RMSD value of 1.628 Å was a measure of the difference between the pose predicted by the docking program and the experimentally determined X-ray crystal structure. In this study, an RMSD of 1.628 Å suggests that the docking program is reliable for predicting the binding mode of Strychnine to TAS2R46. The binding energy of -6.96 kcal/mol and the inhibition constant (Ki) of 7.89 µM provide further insights into the quality of the docking results. A lower binding energy is generally indicative of a more favorable interaction, and the Ki value represents the concentration at which 50% of the receptor sites are occupied. These values suggest a strong binding affinity between strychnine and TAS2R46.

Binding energy
The binding energy (ΔG) of 19 volatile compounds in coconut shell liquid smoke in the binding site of the TAS2R46 macromolecule (PDB ID 7XP6) was calculated using AutoDock 4.2 software (Table 1). These binding energies were indicative of the strength of interaction between the ligands and the receptor. Additionally, the inhibition constant (Ki) values can be derived from these ΔG values, providing insight into the ligands' affinities for the receptor.

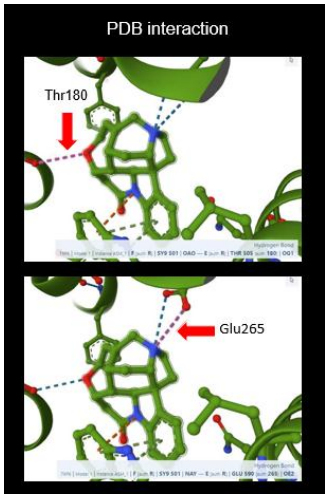

a

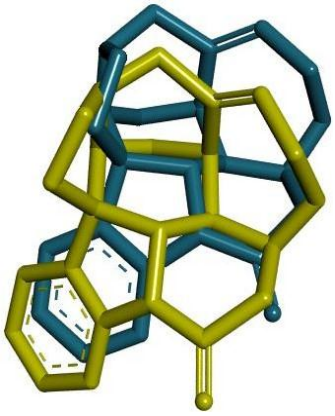
b

Figure 1: Visualization of re-docking of the native ligand (strychnine) into the binding site of the human bitter taste TAS2R46 macromolecule (PDB ID 7XP6). The binding mode of strychnine from X-ray crystallography (a). Overlaying of the native ligand X-ray crystallography (Green) and native ligand resulting from re-docking (Blue) (b).

Table 1: Binding of energy for 19 volatile compounds in coconut shell liquid smoke in the binding site of the TAS2R46 macromolecule (PDB ID 7XP6)

Ligand	Binding Energy, ΔG (kcal/mol)	Protein-ligand interactions	
		Number of hydrogen bond	Amino acid residues
Strychnine	-6.96	2	Glu265, Asn184
3-methyl-2-cyclopenten-1-one	-4.04	1	Trp88
2-hydroxymethylphenol	-4.93	4	Asn184, Tyr241, Asn96
2-furanmethanol	-3.60	3	Asn96, Asn184, Tyr241
2-hydroxy-3-methyl-2-cyclopenten-1-one	-4.41	3	Asn92, Asn184
2-methoxyphenol	-4.63	2	Asn184, Asn96
3-methylphenol	-4.58	2	Asn96, Asn92
2-methoxyphenol	-4.63	1	Asn184
2-methoxy-4-methylphenol	-5.08	2	Asn184, Asn96
1,2-benzenediol	-4.68	2	Asn184
3-methoxybenzene-1,2-diol	-4.90	3	Asn184, Trp88
4-ethyl-2-methoxyphenol	-5.30	2	Asn184, Asn92
4-methyl-1,2-benzenediol	-5.10	2	Asn184
2,6-dimethoxyphenol	-4.77	2	Asn184, Asn96
3,4-dimethoxyphenol	-5.11	4	Asn92, Asn96, Trp88, Phe269
4-ethyl-benzene-1,3-diol	-5.14	3	Asn92, Asn96, Trp88
1,2,3-trimethoxybenzene	-4.63	3	Asn92, Trp88, Asn96
1-(2,4,6-trihydroxyphenyl)-ethanone	-5.58	5	Ala268, Asn96, Asn92, Trp88
1,2,3-trimethoxy-5-methylbenzene	-5.03	2	Glu265, Phe269
1-(4-hydroxy-3-methoxyphenyl)-propan-2-one	-5.52	5	Asn184, Phe269, Glu265

ISSN 2616-0684 (Print)
ISSN 2616-0692 (Electronic)

Binding energy (ΔG) represents the free energy of binding, indicating the strength of the interaction between a ligand and its receptor. A lower ΔG value indicates a more favorable and stronger binding interaction. Strychnine has the most negative ΔG of -6.96 kcal/mol, suggesting it forms the strongest interaction with TAS2R46. 2-hydroxymethylphenol has a binding energy that is somewhat less negative than strychnine, indicating a slightly weaker binding affinity. While it's not as strong as strychnine, it still exhibits a reasonably favorable interaction with the receptor. 2-hydroxy-3-methyl-2-cyclopenten-1-one (ΔG = -4.41 kcal/mol) also has a binding energy that was less negative than strychnine, suggesting a weaker binding interaction. However, it's noteworthy that it falls within a similar range of binding affinity as 2-hydroxymethylphenol. 2-methoxy-4-methylphenol (ΔG = -5.08 kcal/mol) has a binding energy that was closer to that of strychnine compared to the previous two ligands. This indicates a stronger binding affinity for TAS2R46. While not as strong as strychnine, it falls within the group of ligands with relatively higher binding affinities in these ligands. Among these three ligands, 2-methoxy-4-methylphenol stands out as having the binding energy closest to that of Strychnine, suggesting a relatively strong binding affinity for TAS2R46. 2-hydroxymethylphenol and 2-hydroxy-3-methyl-2-cyclopenten-1-one have slightly weaker binding affinities, but they still demonstrate favorable interactions with the receptor. In detail, the probability of a given interaction between the receptor and strychnine has been analyzed by examining the interactions on each frame and then averaging the number of occurrences of the interactions on the entire number of frames, as done previously.[19]

Protein-ligand interactions

The protein-ligand interactions in the binding site of the TAS2R46 receptor (PDB ID 7XP6) for various ligands (Figure 2). These interactions are primarily characterized by the number of hydrogen bonds formed and the specific amino acid residues involved. Strychnine formed 2 hydrogen bonds with the receptor. These bonds involved the amino acid residues Glu265 and Asn184.

The presence of hydrogen bonds suggests specific and stable interactions between strychnine and TAS2R46, which contribute to its strong binding affinity. The 1-(2,4,6-trihydroxyphenyl)-ethanone and 1-(4-hydroxy-3-methoxyphenyl)-propan-2-one, exhibit binding energies that were close to that of strychnine, suggesting strong binding interactions with TAS2R46.

The number of hydrogen bonds formed between a ligand and the receptor is a crucial factor in determining binding affinity. More hydrogen bonds generally indicate stronger interactions. Ligands forming multiple hydrogen bonds with key amino acid residues (e.g., Asn184, Trp88, Asn96, Tyr241) are likely to have higher binding affinities. 1-(2,4,6-trihydroxyphenyl)-ethanone and 1-(4-hydroxy-3-methoxyphenyl)-propan-2-one, with 5 hydrogen bonds each, were among the ligands with the most extensive and specific interactions with the receptor. It was discovered that the orthosteric binding site of TAS2Rs aligned with that of class A GPCRs, and the ability of bitter compounds to bind to multiple specificities was accomplished through the utilization of sub-pockets within the orthosteric binding site. This enabled distinct types of interactions to occur with various ligands.[20] These interactions provide insights into the mechanisms of ligand-receptor binding for TAS2R46 and can guide further investigations into the ligands' functional properties and biological effects. These ligands are promising candidates for further experimental studies to confirm their binding interactions and explore their biological effects with TAS2R46. Their relatively strong binding affinities suggest potential functional significance in the context of this receptor.

Molecular dynamics

Molecular dynamics is a computer methodology utilized to model the time-dependent dynamic behavior of molecular systems, under the assumption that all entities within the simulation box possess flexibility.[21,22] It can be used to explore molecular conformations and as a docking method itself. Molecular dynamics simulations can be used before docking to generate an ensemble of protein conformations and after docking to optimize the structures of the final complexes, calculate more detailed interaction energies, and provide information about the ligand binding mechanism.

RMSD

The Root Mean Square Deviation (RMSD) variation of the TAS2R46 protein and its ligand, strychnine, was examined during a molecular dynamics simulation lasting 100 nanoseconds (Figure 3a). RMSD is a valuable metric used in structural biology and computational chemistry to measure the structural deviation of a molecule or complex from its reference structure, providing insights into the stability and dynamics of the system being studied. The RMSD of TAS2R46 fluctuated during the simulation. It started at approximately 0.15 Å and gradually increased until it reached a maximum of around 1.14 Å at t=30 ns. This initial increase suggested that TAS2R46 underwent some structural adjustments during the first 30 ns. After that, its RMSD started to decrease and fluctuated around 0.85-1.14 Å. This indicated that TAS2R46 eventually stabilized in a conformation somewhat different from its initial state but remained relatively consistent. The RMSD of strychnine exhibited different behavior compared to TAS2R46.

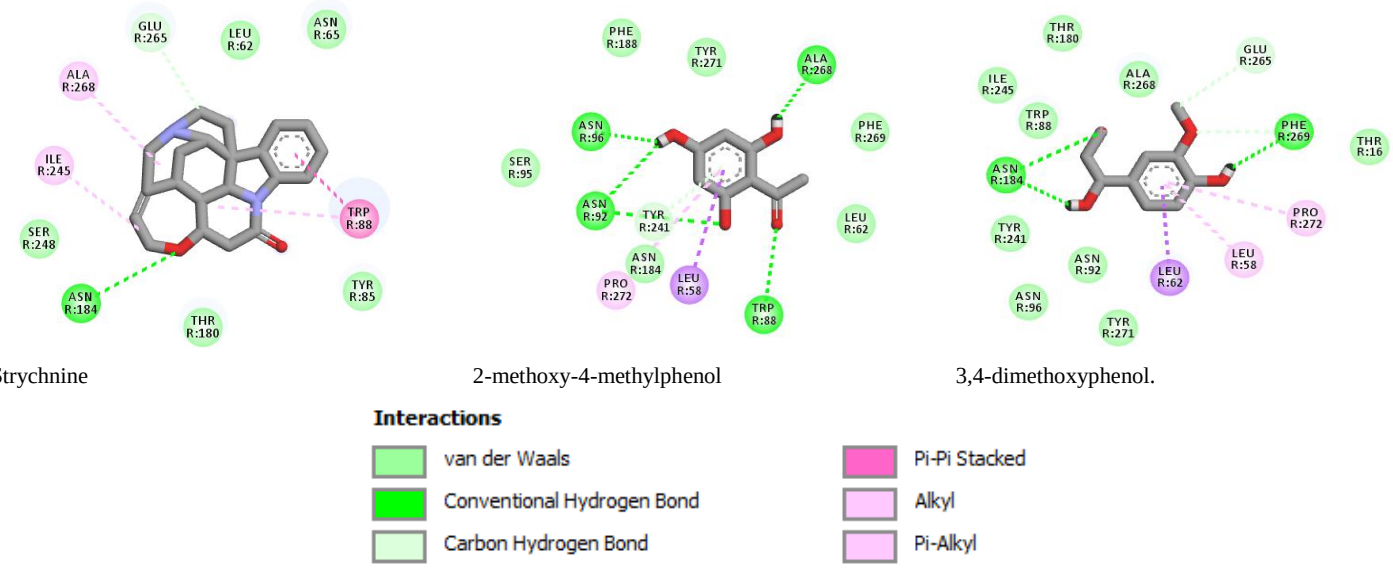

Strychnine 2-methoxy-4-methylphenol 3,4-dimethoxyphenol.

Figure 2: Visualization of 2D interactions for strychnine, 1-(2,4,6-trihydroxyphenyl)-ethanone, and 1-(4-hydroxy-3-methoxyphenyl)-propan-2-one.

ISSN 2616-0684 (Print)
ISSN 2616-0692 (Electronic)

It started at approximately 0.0005 Å and quickly jumped to around 0.227 Å at t=5 ns, indicating a significant deviation from its initial conformation. It continued to fluctuate, reaching a maximum of approximately 0.364 Å at t=35 ns. This suggested that strychnine experienced considerable mobility and flexibility within the binding pocket of TAS2R46.

The observed fluctuations in RMSD values for TAS2R46 and strychnine could be attributed to the dynamics of the protein-ligand complex during the simulation. It was common for proteins to undergo conformational changes in response to ligand binding, and the ligand itself could also exhibit significant flexibility within the binding pocket. The fluctuations in TAS2R46 RMSD may have indicated structural rearrangements necessary for the protein to accommodate strychnine or adapt to the binding interaction. As the simulation progressed, TAS2R46 appeared to reach a relatively stable conformation with a consistent RMSD value, suggesting it had found an energetically favorable binding state. In contrast, the larger and more variable fluctuations in the RMSD of strychnine suggested that the ligand explored various binding conformations during the simulation. This flexibility in strychnine's conformation within the binding pocket was likely reflective of its dynamic interactions with the protein.

In conclusion, the RMSD data for TAS2R46 and strychnine during the 100 ns simulation provided insights into the dynamic behavior of the protein-ligand complex. These fluctuations were expected in molecular dynamics simulations and offered valuable information about the structural dynamics and stability of the system under investigation.

Analyzed for the Root Mean Square Deviation (RMSD) fluctuation of the TAS2R46 protein and 1-(2,4,6-trihydroxyphenyl)-ethanone, over a 100 ns molecular dynamics simulation (Fig. 3b). The RMSD of TAS2R46 fluctuated during the simulation. It started at approximately 0.17 Å and experienced a gradual increase, reaching a maximum of around 1.17 Å at t=95 ns. This suggests that TAS2R46 underwent significant structural changes during the simulation. The increasing RMSD values may indicate dynamic conformational adjustments in the protein, reflecting its response to the presence of the 1-(2,4,6-trihydroxyphenyl)-ethanone. The RMSD of 1-(2,4,6-trihydroxyphenyl)-ethanone also exhibited fluctuations during the simulation. It started at a very low value (0.0005 Å) and gradually increased over time, reaching a maximum of approximately 0.68 Å at t=10 ns. The RMSD values for 1-(2,4,6-trihydroxyphenyl)-ethanone remained relatively stable around 0.6-0.7 Å for the remainder of the simulation. This suggests that 1-(2,4,6-trihydroxyphenyl)-ethanone explored different conformations within the binding pocket of TAS2R46 during the initial phase of the simulation but eventually reached a relatively stable binding conformation.

The observed RMSD fluctuations in TAS2R46 and 1-(2,4,6-trihydroxyphenyl)-ethanone reflect the dynamic behavior of the protein-ligand complex during the 100 ns simulation. These fluctuations are typical in molecular dynamics simulations, as proteins and ligands often undergo structural changes to optimize binding interactions. The increasing RMSD in TAS2R46 indicates that the protein undergoes significant conformational adjustments to accommodate 1-(2,4,6-trihydroxyphenyl)-ethanone during the simulation. This adaptation may involve changes in the binding pocket, side-chain movements, or domain reorientations, all of which are common in ligand-protein interactions. The relatively high RMSD value of TAS2R46 at t=95 ns might imply a dynamically stable state for the protein-ligand complex. In contrast, the RMSD fluctuations for 1-(2,4,6-trihydroxyphenyl)-ethanone, with an initial spike followed by stabilization, suggest that the ligand initially explored different binding conformations but eventually settled into a stable conformation within the binding pocket of TAS2R46. Overall, the RMSD data provide valuable insights into the dynamic interactions between TAS2R46 and 1-(2,4,6-TRIHYDROXYPHENYL)-ETHANONE during the simulation, shedding light on the structural dynamics and the stability of the complex.

Analyze the Root Mean Square Deviation (RMSD) fluctuation of the TAS2R46 protein and 1-(4-hydroxy-3-methoxyphenyl)-propan-2-one, over a 100 ns molecular dynamics simulation (Fig. 3c). RMSD is a fundamental metric used in structural biology and computational chemistry to evaluate the structural deviation of a molecule or complex from its reference structure, providing insights into the stability and dynamics of the system. The RMSD of TAS2R46 fluctuated during the simulation. It started at approximately 0.15 Å and displayed a moderate increase until t=40 ns, where it reached around 1.37 Å. This suggests that TAS2R46 experienced significant conformational changes or structural adjustments during this period. Afterward, the RMSD decreased, indicating some degree of stabilization. However, it is important to note that TAS2R46 still exhibited fluctuations in RMSD throughout the simulation. The RMSD of 1-(4-hydroxy-3-methoxyphenyl)-propan-2-one exhibited considerable fluctuations during the simulation. It started at a very low value (0.0005 Å) and rapidly increased to over 1 Å at t=5 ns. This suggests a substantial departure from the initial binding conformation of 1-(4-hydroxy-3-methoxyphenyl)-propan-2-one. Throughout the simulation, the RMSD of 1-(4-hydroxy-3-methoxyphenyl)-propan-2-one showed periodic fluctuations. It reached a maximum of approximately 1.43 Å at t=10 ns and then showed variations around 0.4-1.32 Å. These fluctuations indicate that 1-(4-hydroxy-3-methoxyphenyl)-propan-2-one explored different binding conformations within the binding pocket of TAS2R46.

The observed fluctuations in the RMSD values of TAS2R46 and 1-(4-hydroxy-3-methoxyphenyl)-propan-2-one provide insights into the dynamic behavior of the protein-ligand complex during the 100 ns simulation. These fluctuations are typical in molecular dynamics simulations, reflecting the dynamic nature of protein-ligand interactions.

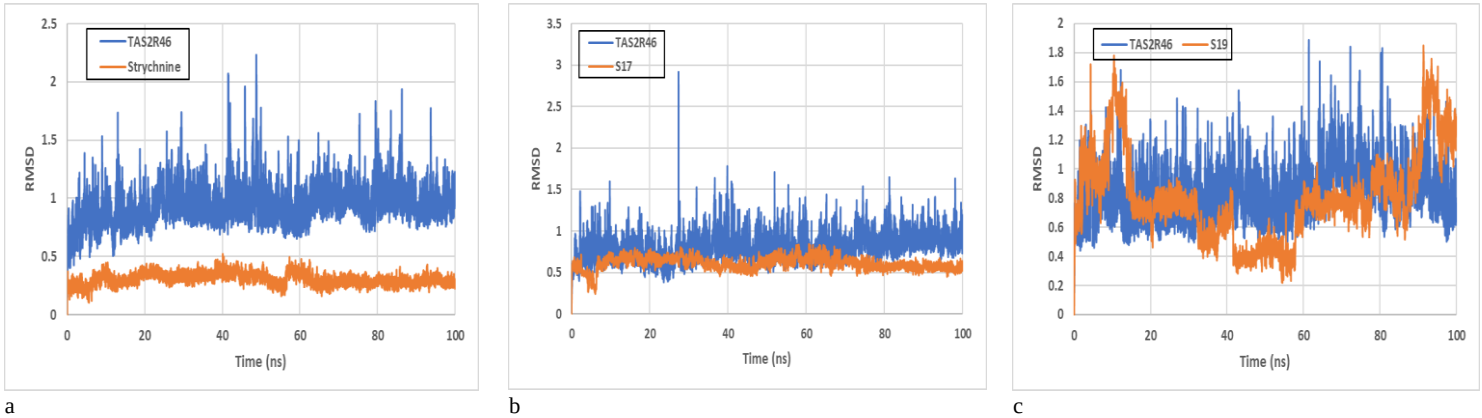

a b c

Figure 3: RMSD fluctuation for strychnine (a), 1-(2,4,6-trihydroxyphenyl)-ethanone (b), and 1-(4-hydroxy-3-methoxyphenyl)-propan-2-one (c).

The increasing RMSD in TAS2R46 suggests that the protein underwent substantial conformational adjustments during the initial phase of the simulation, likely in response to the binding of 1-(4-hydroxy-3-methoxyphenyl)-propan-2-one. The subsequent decrease in RMSD implies that the protein reached a more stable conformation, albeit with fluctuations, which may indicate a dynamically stable state for the protein-ligand complex.

In contrast, the RMSD fluctuations of 1-(4-hydroxy-3-methoxyphenyl)-propan-2-one indicate that the ligand explored different binding conformations within the binding pocket of TAS2R46. The large initial spike in RMSD highlights the ligand's flexibility and the conformational changes it underwent upon binding. Subsequently, the RMSD of 1-(4-hydroxy-3-methoxyphenyl)-propan-2-one displayed variations, suggesting that it continued to sample different binding modes. Overall, the RMSD data provide valuable insights into the dynamic interactions between TAS2R46 and 1-(4-hydroxy-3-methoxyphenyl)-propan-2-one during the simulation, shedding light on the structural dynamics and the stability of the complex.

Three distinct ligands were examined in terms of their Root Mean Square Deviation (RMSD) values: strychnine, 1-(2,4,6-trihydroxyphenyl)-ethanone, and 1-(4-hydroxy-3-methoxyphenyl)-propan-2-one, from a 100 ns molecular dynamics simulation. RMSD is a fundamental metric used in structural biology and computational chemistry to assess the structural deviation of a molecule from its reference structure, providing insights into the stability and dynamics of the ligand in the binding pocket of a protein.

Strychnine, 1-(2,4,6-trihydroxyphenyl)-ethanone, and 1-(4-hydroxy-3-methoxyphenyl)-propan-2-one all experienced fluctuations in RMSD, indicating that they underwent dynamic interactions with the TAS2R46 protein during the simulation. Strychnine exhibited the smallest fluctuations in RMSD, indicating a relatively stable binding to the protein. This suggested a well-defined and maintained binding mode throughout the simulation. 1-(2,4,6-trihydroxyphenyl)-ethanone displayed more significant fluctuations in RMSD, suggesting that it explored a range of binding conformations within the binding pocket of TAS2R46. This could indicate a more dynamic binding interaction. 1-(4-hydroxy-3-methoxyphenyl)-propan-2-one exhibited the most substantial RMSD fluctuations, indicating that it underwent considerable structural changes within the binding pocket, suggesting a highly dynamic binding mode.

In summary, the RMSD data for the three ligands, strychnine, 1-(2,4,6-trihydroxyphenyl)-ethanone, and 1-(4-hydroxy-3-methoxyphenyl)-propan-2-one, provided insights into their dynamic interactions with the TAS2R46 protein during the 100 ns simulation. the extent of RMSD fluctuations varied, reflecting differences in the stability and flexibility of their binding interactions. further analysis, such as clustering or principal component analysis, could offer a more detailed understanding of the structural transitions and conformational changes in these ligand-protein complexes.

RMSF

In the analysis of the Root Mean Square Fluctuation (RMSF) profiles of amino acid residues within the active site of the TAS2R46 protein (PDB ID 7XP6) with the presence of three different ligands (Fig. 4). The RMSF profiles of the amino acid residues in the active site for all three ligands, strychnine, 1-(2,4,6-trihydroxyphenyl)-ethanone, and 1-(4-hydroxy-3-methoxyphenyl)-propan-2-one, were found to be remarkably similar. This suggested that the ligands interacted with the same set of amino acid residues in the active site, causing similar fluctuations in these residues. All three ligands caused significant fluctuations in residue 37, indicating that this residue was involved in stable contact with the ligands. This implied that residue 37 played a critical role in ligand binding and recognition in TAS2R46. Similar to residue 37, residue 75 also exhibited substantial RMSF fluctuations for all three ligands, suggesting that residue 75 was actively involved in binding interactions with strychnine, 1-(2,4,6-trihydroxyphenyl)-ethanone, and 1-(4-hydroxy-3-methoxyphenyl)-propan-2-one. Residue 114 showed high RMSF values, indicating that it was highly flexible, and its fluctuations were consistent across all ligands. This suggested that residue 114 was involved in accommodating the structural changes that occurred during ligand binding. Residue 216 exhibited the highest RMSF values among the analyzed residues. The pronounced fluctuations suggested that residue 216 was very flexible and might undergo significant conformational changes during ligand binding. This residue likely played a key role in the ligand-induced structural rearrangements within the active site. Residue 255 displayed moderate fluctuations in response to all three ligands, indicating that this residue was involved in stable but not highly dynamic interactions with the ligands, contributing to the stability of the binding site. Similar to residue 255, residue 301 also showed moderate RMSF values, indicating that residue 301 was involved in stable but not highly flexible contacts with the ligands and contributed to the overall stability of the active site.

The similarity in RMSF profiles for strychnine, 1-(2,4,6-trihydroxyphenyl)-ethanone, and 1-(4-hydroxy-3-methoxyphenyl)-propan-2-one implied that these ligands comparably interacted with TAS2R46. The highly fluctuating residues, such as 37, 75, and 216, suggested their critical roles in ligand recognition, binding, and potential induced conformational changes. On the other hand, residues 255 and 301 were less dynamic, indicating their contribution to the stable binding environment within the active site.

MMGBSA

The stability of ligands within a protein's active site is often evaluated based on various energy components, which provide insights into the binding interactions. A comprehensive analysis of strychnine, 1-(2,4,6-trihydroxyphenyl)-ethanone, and 1-(4-hydroxy-3-methoxyphenyl)-propan-2-one stability was conducted by examining various energy components, including ΔVDWAALS, ΔEEL, ΔEGB, ΔESURF, ΔGGAS, ΔGSOLV, and ΔTOTAL (Figure 5).

ΔVDWAALS for strychnine was -48.62 kcal/mol, indicating strong Van der Waals interactions with the active site of TAS2R46. Both 1-(2,4,6-trihydroxyphenyl)-ethanone and 1-(4-hydroxy-3-methoxyphenyl)-propan-2-one exhibited significantly lower ΔVDWAALS values (-24.33 and -24.11 kcal/mol, respectively), suggesting weaker Van der Waals interactions with the protein. The ΔEEL for strychnine was -1.43 kcal/mol, suggesting a favorable electrostatic interaction with TAS2R46. 1-(2,4,6-trihydroxyphenyl)-ethanone exhibited a less favorable ΔEEL of -6.88 kcal/mol, indicating weaker electrostatic interactions. 1-(4-hydroxy-3-methoxyphenyl)-propan-2-one had an intermediate ΔEEL value of -2.24 kcal/mol, reflecting moderate electrostatic interactions.

ΔEGB (Electrostatic Interaction with Solvent) was 10.42 for strychnine, suggesting a significant electrostatic interaction with the surrounding solvent. Both 1-(2,4,6-trihydroxyphenyl)-ethanone and 1-(4-hydroxy-3-methoxyphenyl)-propan-2-one displayed ΔEGB values (14.52 and 9.94 kcal/mol, respectively) indicating relatively stronger electrostatic interactions with the solvent compared to strychnine.

ΔESURF (Nonpolar Solvation Energy) for strychnine was -4.24 kcal/mol, indicating a favorable nonpolar solvation effect. Both 1-(2,4,6-trihydroxyphenyl)-ethanone and 1-(4-hydroxy-3-methoxyphenyl)-propan-2-one had similar ΔESURF values (-3.61 and -3.42 kcal/mol), suggesting comparable nonpolar solvation effects. ΔGGAS (Gas Phase Energy) was -50.05 kcal/mol for strychnine, reflecting its overall gas phase energy during binding. Both 1-(2,4,6-trihydroxyphenyl)-ethanone and 1-(4-hydroxy-3-methoxyphenyl)-propan-2-one had higher ΔGGAS values (-31.21 and -26.35 kcal/mol), indicating that they were less stable in the gas phase compared to strychnine.

ΔGSOLV (Solvation Energy) was 6.19 kcal/mol, indicating a favorable solvation energy for strychnine. Both 1-(2,4,6-trihydroxyphenyl)-ethanone and 1-(4-hydroxy-3-methoxyphenyl)-propan-2-one showed similar ΔGSOLV values (10.91 and 6.51 kcal/mol), suggesting comparable solvation effects. ΔTOTAL (Total Energy) was -43.87 kcal/mol, representing the overall energy contribution for strychnine's stability in the active site. Both 1-(2,4,6-trihydroxyphenyl)-ethanone and 1-(4-hydroxy-3-methoxyphenyl)-propan-2-one had less negative ΔTOTAL values (-20.3 and -19.84 kcal/mol), indicating that they were less stable in the active site compared to strychnine.

ISSN 2616-0684 (Print)
ISSN 2616-0692 (Electronic)

The analysis of these energy components suggests that strychnine exhibited stronger Van der Waals interactions and more favorable electrostatic interactions with TAS2R46 compared to 1-(2,4,6-trihydroxyphenyl)-ethanone and 1-(4-hydroxy-3-methoxyphenyl)-propan-2-one. Additionally, strychnine demonstrated better stability in the gas phase, more favorable nonpolar solvation energy, and relatively more favorable total energy, indicating its strong binding within the active site. In contrast, 1-(2,4,6-trihydroxyphenyl)-ethanone and 1-(4-hydroxy-3-methoxyphenyl)-propan-2-one showed weaker interactions and less stability in these various energy components, suggesting that may have less favorable binding within the active site.
Bitter taste perception is predicated on bitter taste receptors (TAS2Rs), however, mounting data suggests that bitter taste receptors are also produced in a variety of extra-oral tissues. Generally, the activation of these extra-oral TAS2Rs induces signals and cellular responses that are location-dependent and crucial for metabolism and homeostasis.[23] By combining network-based methods with MD simulations, the study distinguishes between the active and inactive conformational states of the bitter taste receptor TAS2R46 in humans. Furthermore, an examination is conducted into the molecular mechanisms that govern the flow of information between the EC and IC regions. The dynamical characteristics of active and inactive TAS2R46 states are illuminated in this study, which also identifies possible signal transfer pathways from the orthosteric binding site to G-protein-coupled areas.[24]

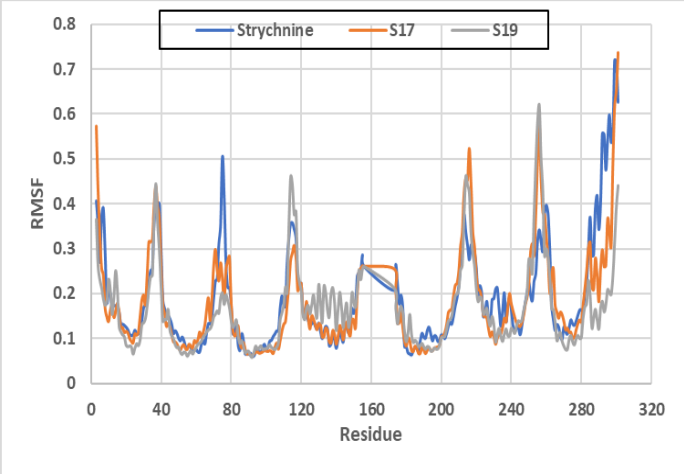

Figure 4: RMSF fluctuation for strychnine (blue), 1-(2,4,6-trihydroxyphenyl)-ethanone (orange), and 1-(4-hydroxy-3-methoxyphenyl)-propan-2-one (grey).

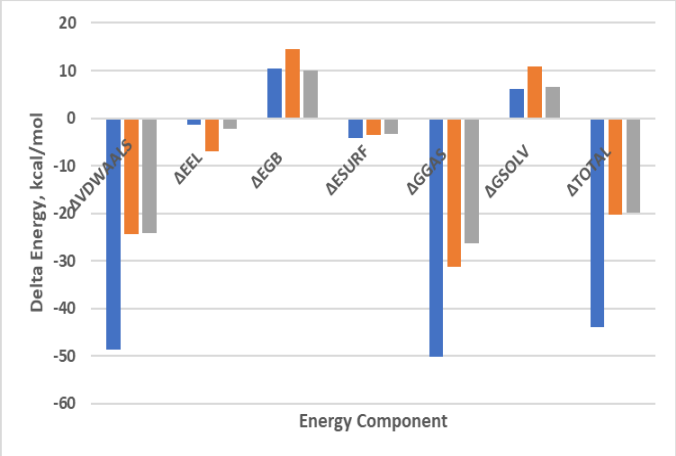

Figure 5: Energy component for strychnine (blue), 1-(2,4,6-trihydroxyphenyl)-ethanone (orange), and 1-(4-hydroxy-3-methoxyphenyl)-propan-2-one (grey).

Conclusion

Exploring the mechanism of liquid smoke perception and its interaction with the human bitter taste receptor TAS2R46 (PDB ID 7XP6) through molecular docking and molecular dynamics simulations has provided valuable insights into the potential binding modes, stability, and dynamics of this interaction. Molecular docking results indicated that all the volatile compounds of liquid smoke were capable of binding to the TAS2R46 receptor. This suggests that liquid smoke compounds are potential ligands for TAS2R46. Molecular dynamics simulations provided insights into the stability and dynamics of the TAS2R46-liquid smoke ligand complexes. 1-(2,4,6-trihydroxyphenyl)-ethanone, the closer ligand to strychnine, exhibited the most negative delta energy component, suggesting the most stable binding to TAS2R46. These findings can guide further studies in the field of taste perception and may have applications in the food industry and drug discovery. Further experimental validation will be essential to confirm and extend these computational results, providing a comprehensive understanding of the interaction between TAS2R46 and bitter compounds in liquid smoke.

Conflict of Interest

The authors declare no conflict of interest.

Authors' Declaration

The authors hereby declare that the work presented in this article is original and that any liability for claims relating to the content of this article will be borne by them.

References

1. Jelena M, Zorana M. Flavors, colors, and preservatives used in processed cheese. In: Processed Cheese Science and Technology. Elsevier; 2022. P. 125-47.
2. Xin X, Dell K, Udugama IA, Young BR, Baroutian S. Transforming biomass pyrolysis technologies to produce liquid smoke food flavouring. J Clean Prod 2021;294:125368.
3. Racioppo A, Speranza B, Pilone V, Stasi A, Mocerino E, Scognamiglio G, et al. Optimizing liquid smoke conditions for the production and preservation of innovative fish products. Food Biosci 2023;53:102712.
4. Petridis D, Zotos A, Kampouris T, Roumelioti Z. Optimization of a steaming with liquid smoke smoking process of Mediterranean mussel (Mytilus galloprovincialis). Food Sci Technol Int 2013;19(1):59-68.
5. Hadanu R, Apituley DAN. Volatile Compounds Detected in Coconut Shell Liquid Smoke through Pyrolysis at a Fractioning Temperature of 350-420 C. Makara J Sci Published online 2016:95-100.
6. Mulyawanti I, Kailaku S, Syah A. Chemical identification of coconut shell liquid smoke. In: Vol 309. IOP Publishing; 2019. P. 012020.
7. Surboyo MDC, Arundina I, Rahayu RP, Mansur D, Bramantoro T. Potential of distilled liquid smoke derived from coconut (Cocos nucifera L) shell for traumatic ulcer healing in diabetic rats. Eur J Dent 2019;13(02):271-9.
8. Behrens M, Meyerhof W. Mammalian bitter taste perception. Chemosens Syst Mamm Fishes Insects Published online 2009:77-96.
9. Zhang Y, Hoon MA, Chandrashekar J, Mueller KL, Cook B, Wu D, Zuker CS, Ryba NJP. Coding of sweet, bitter, and umami tastes: different receptor cells sharing similar signaling pathways. Cell 2003;112(3):293-301.
10. Ahmad R, Dalziel JE. G protein-coupled receptors in taste physiology and pharmacology. Front Pharmacol 2020;11:587664.
11. Jaggupilli A, Singh N, Upadhyaya J, Sikarwar AS, Arakawa M, Dakshinamurti S, Bhullar RP, Duan K, Chelikani P.

Analysis of the expression of human bitter taste receptors in extraoral tissues. Mol Cell Biochem 2017;426:137-47.
12. Hu K, Chang R, Zhu Q, Wan J, Tang P, Liu C, et al. Exploring the mechanism of liquid smoke and human taste perception based on the synergy of the electronic tongue, molecular docking, and multiple linear regression. Food Biophys 2020;15:482-94.
13. Acevedo W, González-Nilo F, Agosin E. Docking and molecular dynamics of steviol glycoside–human bitter receptor interactions. J Agric Food Chem 2016;64(40):7585-96.
14. Dallakyan S, Olson AJ. Small-molecule library screening by docking with PyRx. Chem Biol Methods Protoc Published online 2015:243-50.
15. Snyder HD, Kucukkal TG. Computational chemistry activities with Avogadro and ORCA. J Chem Educ 2021;98(4):1335-41.
16. Jejurikar BL, Rohane SH. Drug designing in discovery studio. Published online 2021.
17. Xu W, Wu L, Liu S, Liu X, Cao X, Zhou C, Zhang J, Fu Y, Guo Y, Wu Y, Tan Q, Wang L, Liu J, Jiang L, Fan Z, Pei Y, Yu J, Cheng J, Zhao S, Hao X, Liu ZJ, Hua T. Structural basis for strychnine activation of human bitter taste receptor TAS2R46. Science 2022;377(6612):1298-304.
18. Talmon M, Massara E, Quaregna M, De Battisti M, Boccafoschi F, Lecchi G, Puppo F, Cajandab MAB, Salamone S, Bovio E, Boldorini R, Riva B, Pollastro F, Fresu LG. Bitter taste receptor (TAS2R) 46 in human skeletal muscle: expression and activity. Front Pharmacol 2023;14.
19. Miceli M, Deriu MA, Grasso G. Toward the design and development of peptidomimetic inhibitors of the Ataxin-1 aggregation pathway. Biophys J 2022;121(23):4679-88.
20. Nowak S, Di Pizio A, Levit A, Niv MY, Meyerhof W, Behrens M. Reengineering the ligand sensitivity of the broadly tuned human bitter taste receptor TAS2R14. Biochim Biophys Acta BBA-Gen Subj 2018;1862(10):2162-73.
21. Asnawi A, Nedja M, Febrina E, Purwaniati P. Prediction of a Stable Complex of Compounds in the Ethanol Extract of Celery Leaves (Apium graveolens L.) Function as a VKORC1. Trop J Nat Prod Res. 2023;7(2):2362-70.
22. Febrina E, Asnawi A. Lead compound discovery using pharmacophore-based models of small-molecule metabolites from human blood as inhibitor cellular entry of SARS-CoV-2. J Pharm Pharmacogn Res 2023;11(5):810-22.
23. Pan S, Sharma P, Shah SD, Deshpande DA. Bitter taste receptor agonists alter mitochondrial function and induce autophagy in airway smooth muscle cells. Am J Physiol-Lung Cell Mol Physiol 2017;313(1):L154-65.
24. Cannariato M, Fanunza R, Zizzi EA, Miceli M, Di Benedetto G, Deriu MA, et al. Molecular Biomechanics of the TAS2R46 Bitter Taste Receptor through Network-based Investigation. bioRxiv Published online 2023:2023-11